WFS Entrance Windows acceptance test

Doc. No.	ARGOS Technical Note 109
Issue	1.0
Date	15/04/2011

Prepared	L. Busoni, M. Bonaglia	2011/04/15
	Name	Date

TABLE OF CONTENTS

Change Record

Issue	Date	Section/ Paragraph Affected	Reasons / Remarks	Name
1.0	15.04.2011	all	created	M. Bonaglia

1 Scope.

This document reports the measurements done on the 7 units of Entance Window (EW) produced by Custom Scientific and delivered to INAF – Arcetri Observatory on 01/04/2011. These measurements are aimed to check if the most critical features of the EW are within the manufacturing specifications provided to Custom Scientific (see AD 1).

2 Applicable documents.

No.	Title	File name
AD 1	Wavefront sensor Entrance Window procurement	OAA_EntWin_approved2.doc
AD 2		

3 Introduction.

The ARGOS WFS Entrance windows are composed by 2 elements: the first one is a 4mm thick plane-parallel window drilled in the center of the front surface. The second one is a 6mm thick wedged window. Figure 1 shows the two optical elements that compose the EW.

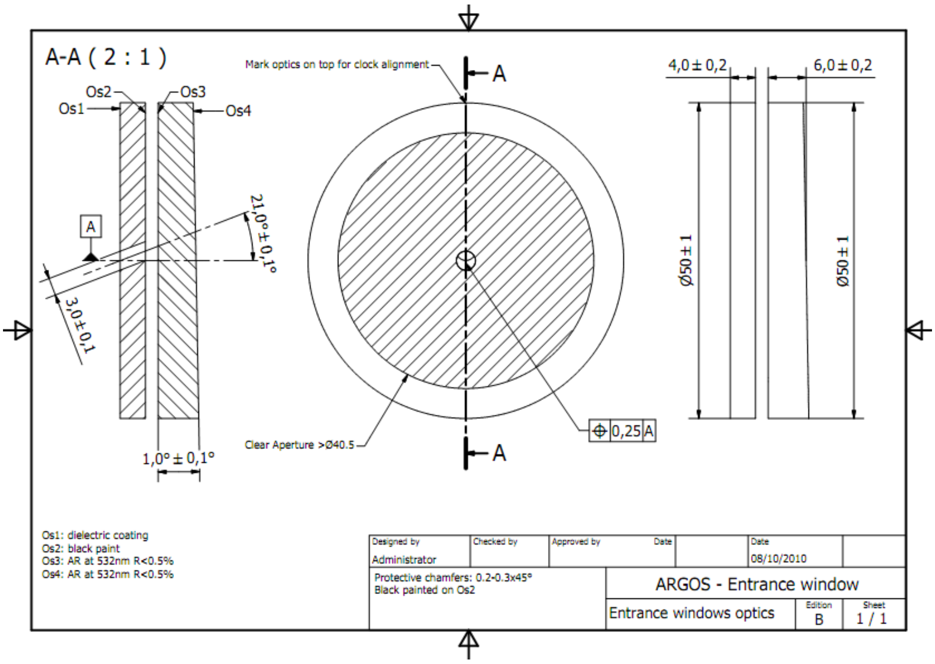

Figure 1. Construction drawning of 1 piece of Entrance Window.

4 Test of the 1st element (reflective plate).

The optical surfaces of the 1st element of the EW have the following specifications:

- OS 1: it is drilled with a thru-hole of (3.0±0.1)mm diameter. The hole axis is inclined by (21.0±0.1)deg with respect to the normal to the OS 1. It is polished to ensure a λ/4 surface quality over the clear aperture. It is dielectric coated to ensure a reflectivity of >95% at 532nm.
- OS 2: the rear surface of the first element of the EW is commercially polished and black-painted to block the few percent of light transmitted from OS 1 to reach the WFS.

The most important features of this element are the position and diameter of the thru-hole. We measured these parameters using different setups and we cross checked the results.

4.1 Test with photographic image.

This test has been done on one element of the 7 units we got from Custom Scientific. We taken a picture of the reflective plate of the Entrance Window (file `IMG_7847.jpg`). The hole center coordinates are (1515; 1182). We first analized the row 1182.

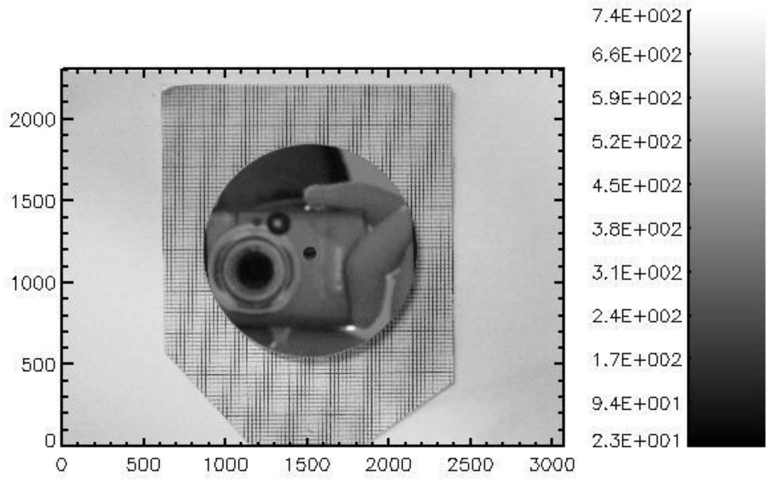

Figure 2. Picture of the reflective plate of the Entrance Window.

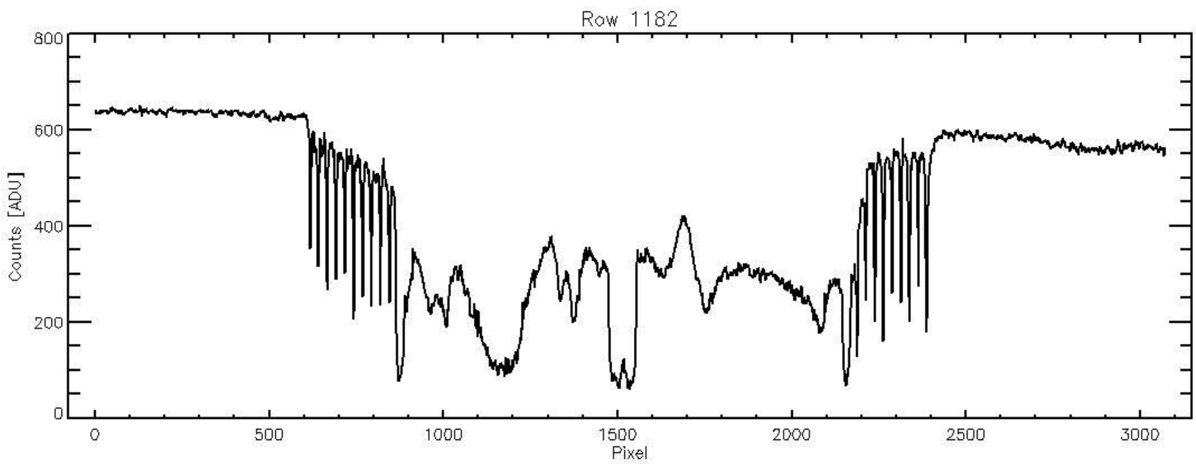

Figure 3. Plot of the row 1182. The different image features are marked.

The pixel scale of the image calculated from the graph paper pattern is (172±2)px/7mm = (24.6±0.3)px/mm.

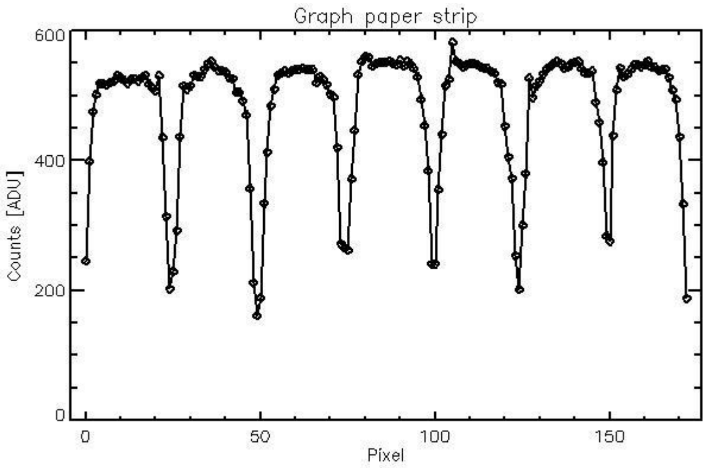

Figure 4. Pattern of the graph paper used to calibrate the image pixel scale.

We calibrated the image pixel scale also comparing the window diameter measured with a caliber. With the caliber the window diameter is (50.92±0.01)mm.

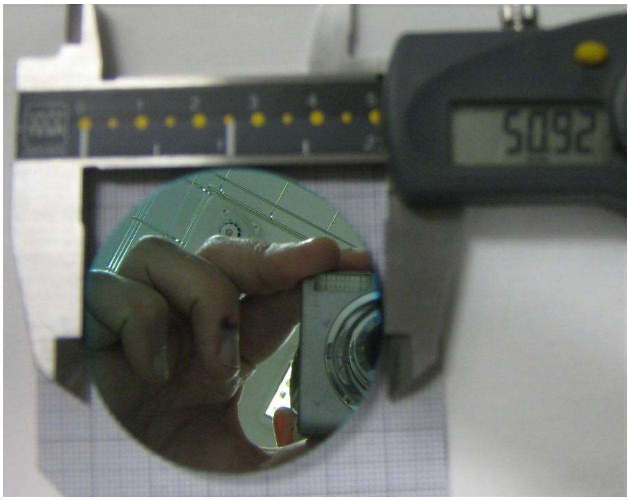

Figure 5. Window diameter measured with the caliber.

In the picture of Figure 2 the window diameter is (1285±2)px. So the image scale calculated is (25.25±0.05)px/mm.
In Figure 2 the measured major and minor axis of the central hole are (84±2)px and (80±2)px corresponding to (3.3±0.1)mm and (3.2±0.1)mm using the pixel scale calibrated from the window diameter. Using the pixel scale calibrated form the graph paper pattern the hole dimensions are (3.4±0.1)mm and (3.2±0.1)mm.

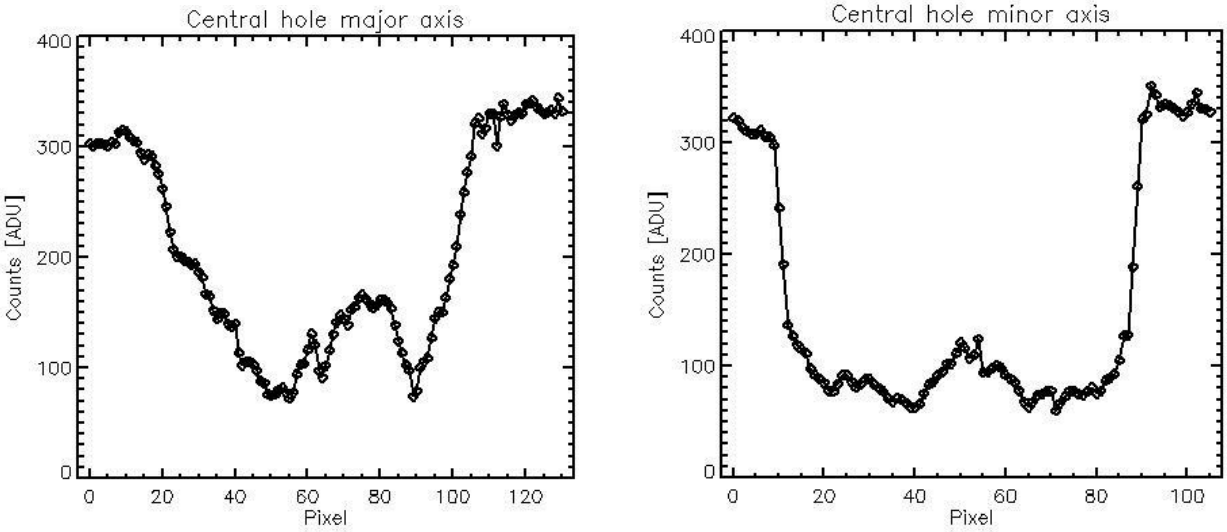

Figure 6. Plot of the cuts thorugh the cental hole axes.

4.2 Test with microscope.

We checked the hole dimension using a microscope and a camera (Prosilica GC1350). We taken two images at different magnifications.

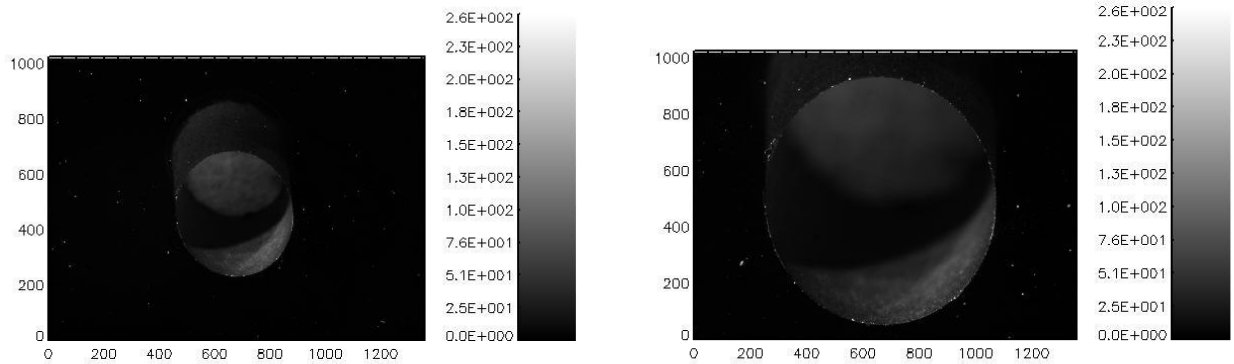

Figure 7. Central hole images taken with the microscope at two magnifications.

To check the pixel scale of the camera connected to the microscope we imaged a graphic paper sheet using the same magnifications and refocussing the camera.

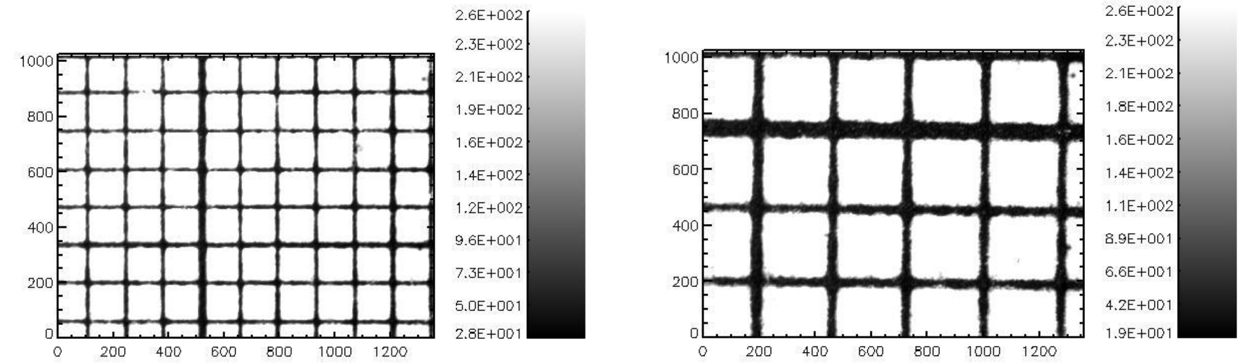

Figure 8. Graph paper used to calibrate the two images pixel scale.

From the first image the pixel scale is (1265±2)px/9mm = (140.5±0.2)px/mm, the second one has a pixel scale of (1080±2)px/4mm = (270.0±0.5)px/mm.

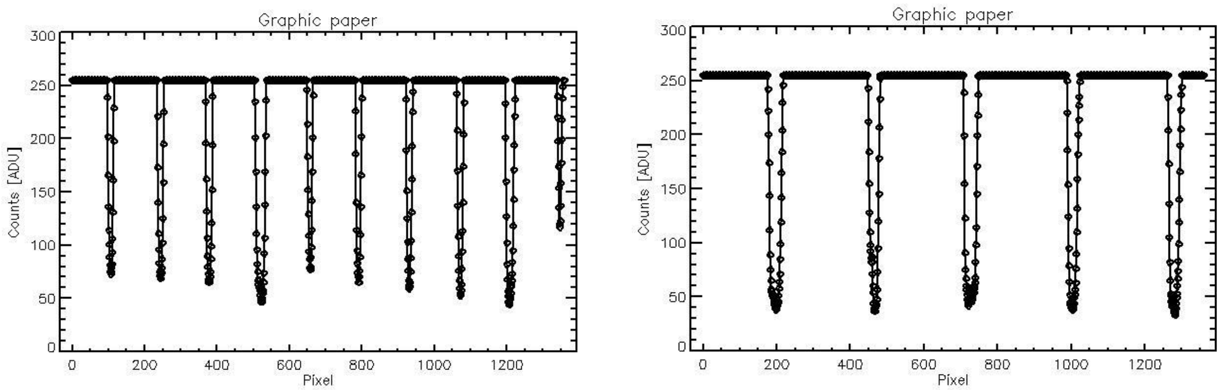

Figure 9. Plot of the graph paper pattern at the two magnifications.

The hole minor axis is (424±2)px = (3.02±0.02)mm in the first image and (824±2)px = (3.05±0.01)mm in the second image.
The hole major axis is (447±2)px = (3.18±0.02)mm in the first image and (875±2)px = (3.24±0.01)mm in the second image.

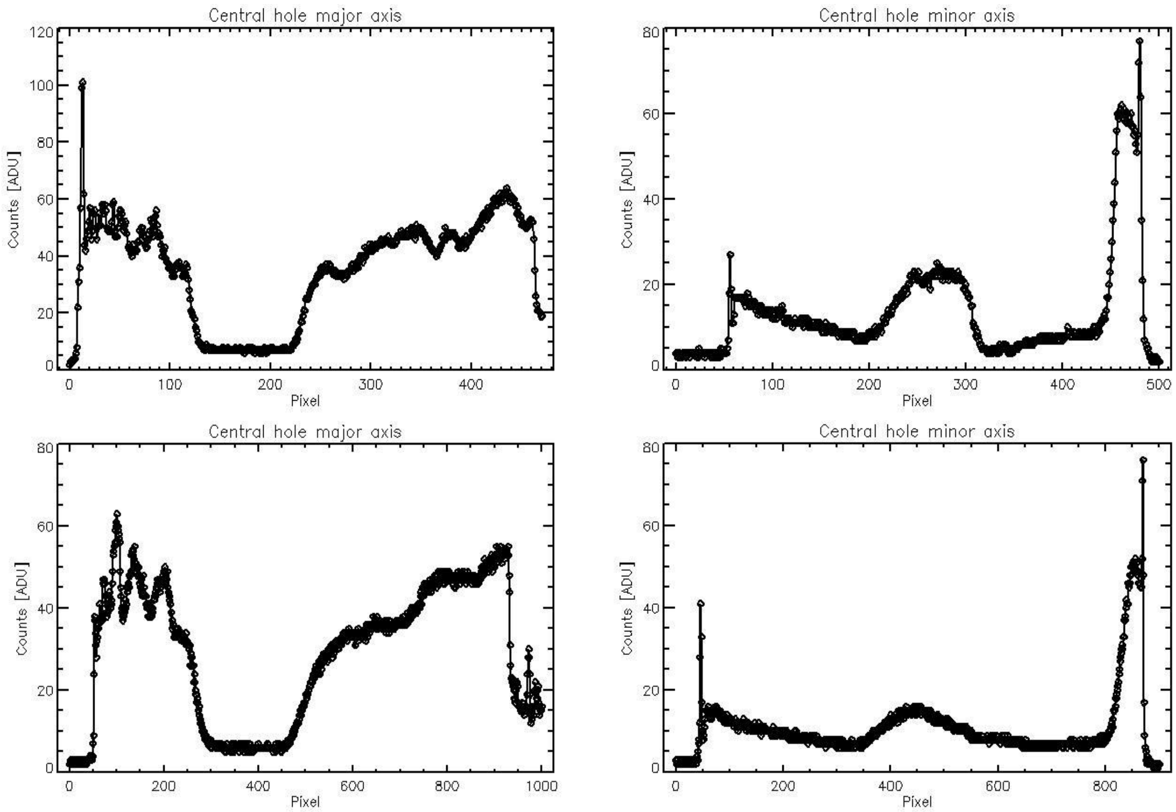

Figure 10. Plots of the major and minor axes of the central hole at the two different magnifications.

4.3 Test with microscope and micrometric translator.

We measured the central hole dimensions also translating the window under the microscope with a micrometer and checking the hole axes lenght with respect a reference point. We measured a minor axis for of (3.04±0.02)mm and a major axis of (3.22±0.02)mm.

4.4 Conclusion.

We resumed the mesurements done on the first window in the table below:

Table 1. Resume of the measurement done.

Measure type	Pixel scale [px/mm]	Major axis [mm]	Minor axis [mm]	Ratio	Inclination [deg]
Picture graph pap.	24.6±0.3	3.4±0.1	3.2±0.1	0.94±0.06	20±1
Picture diam.	25.25±0.05	3.3±0.1	3.2±0.1	0.97±0.06	14.1±0.9
Microscope M1	140.5±0.2	3.18±0.02	3.02±0.02	0.95±0.01	18.2±0.2
Microscope M2	270.0±0.5	3.24±0.01	3.05±0.01	0.941±0.005	20.0±0.1
Microscope + micrometer	-	3.22±0.02	3.04±0.02	0.944±0.01	19.3±0.2

On these results we decided to measure the dimensions of the 7 windows using the last procedure: the microscope with translator. We measured the diameter of the aluminized area and the distances between the central hole and the external edge on the aluminized surface. From these measurements we evaluated the inclination of the hole and the decenter.

Table 2. Measures of the 7 EW dimensions done with microscope and micrometric translator.

EW #	a [mm]	b [mm]	D [mm]	Hole incl [deg]	Dec Y [mm]	Dec X [mm]
0	3,27	3,05	51,11	21,0277	-1,14	0,17
1	3,29	3,08	50,59	20,4757	-0,51	0,09
2	3,25	3,05	51,03	20,1009	-1,43	0,01
3	3,3	3,07	51,14	21,4068	-1,02	0,00
4	3,29	3,08	51,05	20,4757	-1,40	-0,03
5	3,24	3,03	50,85	20,6348	-1,02	-0,04
6	3,27	3,07	50,90	20,0387	-0,97	-0,08

The field stop position for the 7 windows are plotted in figure below, it seems that the holes are -1arcsec decentered in the radial direction:

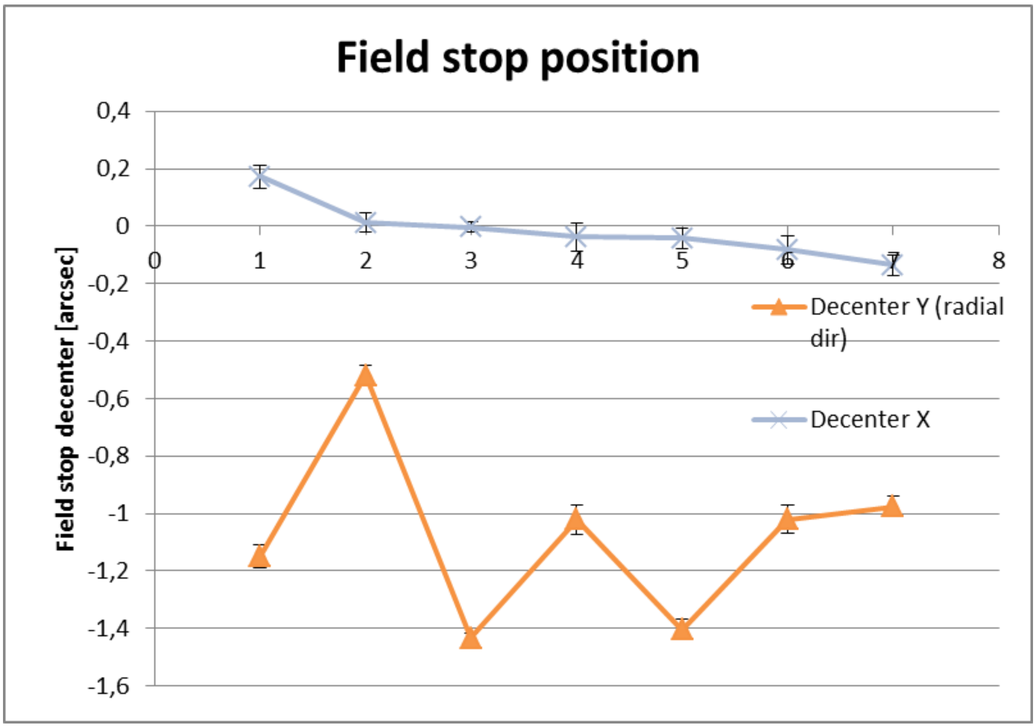

Figure 11. Plot of the field stop position on the aluminized surface of the 7 EW.

The field stop dimension is plotted below, on average the holes are 4.6arcsec wide:

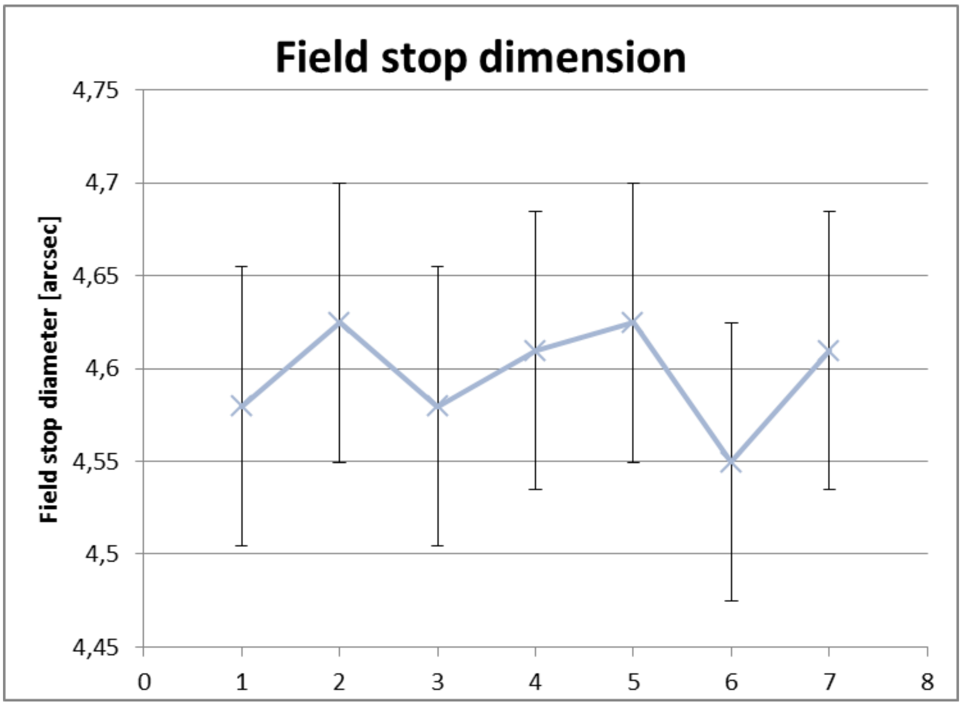

Figure 12. Field stop dimension on the aluminized surface of the 7 EW.

5 Test of the 2nd element (transmissive plate).

This element is a wedged transmissive window. The element is shown in Figure 13. The wedge direction has been marked with an arrow, in correspondence of the thinner edge of the window.
The main specifications for the optical surfaces of the element are:

- OS 3: it is polished to ensure a λ/10 surface quality and it is coated to ensure a T>99.5% at 532nm over a 30mm diameter patch, centered on the optical axis.
- OS 4: same polishing and coating of OS 3. It is wedged by (1.0±0.1)deg with respect to the OS 3.

Figure 13. Picture of the 2nd element of the EW. The arrow visible on the right picture marks the thinner edge of the window.

The critical features of this element are the optical quality in transmission of the window and the inclination of the wedge. These parameters have been tested in laboratory.

5.1 Test of wedge angle.

The setup used to test the wedge angle is shown in Figure 14. We aligned the laser pointer to project a beam parallel to the optical bench. We fixed a rail on the bench and we measured the position of the beam at the beginning and at the end of the rail using a CCD camera (AVT/Prosilica GC1350).

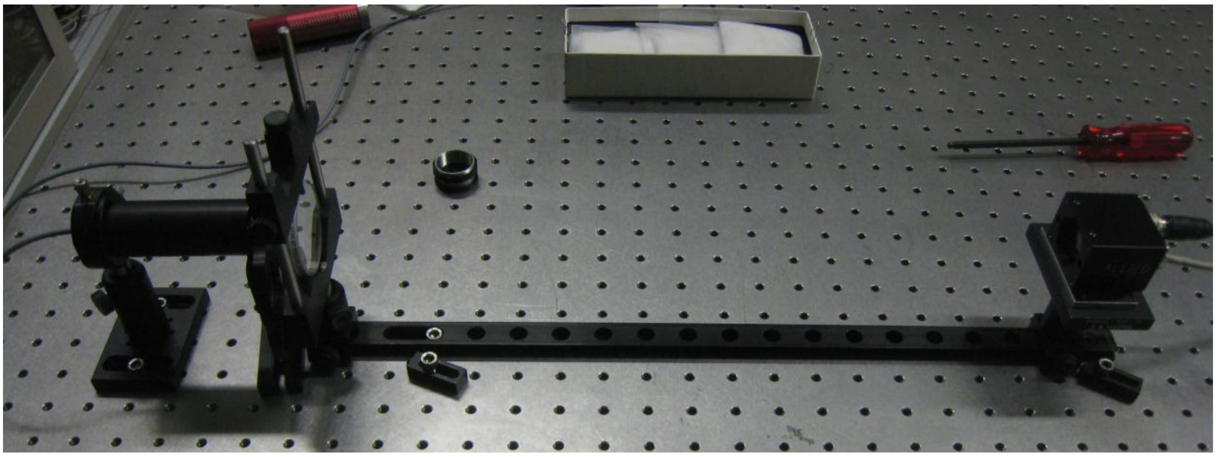

Figure 14. Picture of the setup used to test the wedge angle of the 2nd EW element.

The differential position of the spot has been evaluated averaging 10 frames (dark subtracted) and computing the centroid. We measured a shift of 20µm in the direction perpendicular to the bench over the (405±1)mm lenght of the rail. This means that the beam is tilted by 0.003deg towards the bench.
We positioned the window between the laser source and the beginning of the rail and we acquired again the spot position. Figure 15 shows the two spots at the edges of the rail.

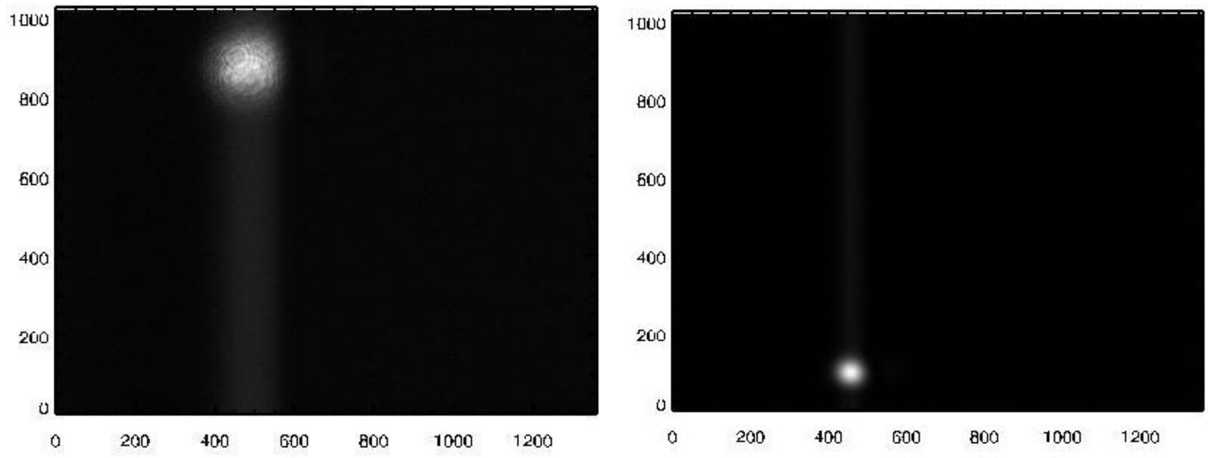

Figure 15. Position of the laser beam on the camera frame at the beginning (left) and at the end (right) of the rail.

The differential position is (788±2)px = (3.66±0.01)mm. Subtracting the 20µm shift of the beam itself this measure means that the outcoming beam is tilted by θ_m = (0.515±0.003)deg with respect the bench plane. The wedge angle has been evaluated using the formula: $n_{BK7} \sin \theta_i = \sin \theta_o$, where θ_i and θ_o are the angles between the normal to the 2 surfaces and the beam and n_{BK7} = 1.51947. Because $\theta_o = \theta_i + \theta_m$ we evaluated θ_i as: $\theta_i = \theta_m / (n_{BK7} - 1)$ = (0.991±0.005)deg. θ_i corresponds to the angle between the two surfaces of the element, so the wedge angle is in specification.

5.2 Test of the optical quality in transmission.

This test has been done using an interferometer (Wyko 4100 RTI) and a reference flat mirror. First we acquired an interferogram of the cavity, then we inserted the window in the optical path and we readjusted the mirror tip and tilt to compensate for the window wedge. We subtracted the interferogram of the cavity to the one of the window + cavity using fiducials. In both cases we masked the detector to analyze the 90% of the window diameter. The results of the analysis are shown in Figure 16, parameters are referred to surface. The window surface quality is better than λ/30 that is compliant with specification.
We also analyzed the windows to check for polishing defects and scratches. This inspection has been done by eye, using an halogen lamp as light source. No visible defects has been seen on all the 7 pieces.

6 Conclusion.

We tested in laboratory the most critical features of the WFS EW. All the parameters checked are in specifications.

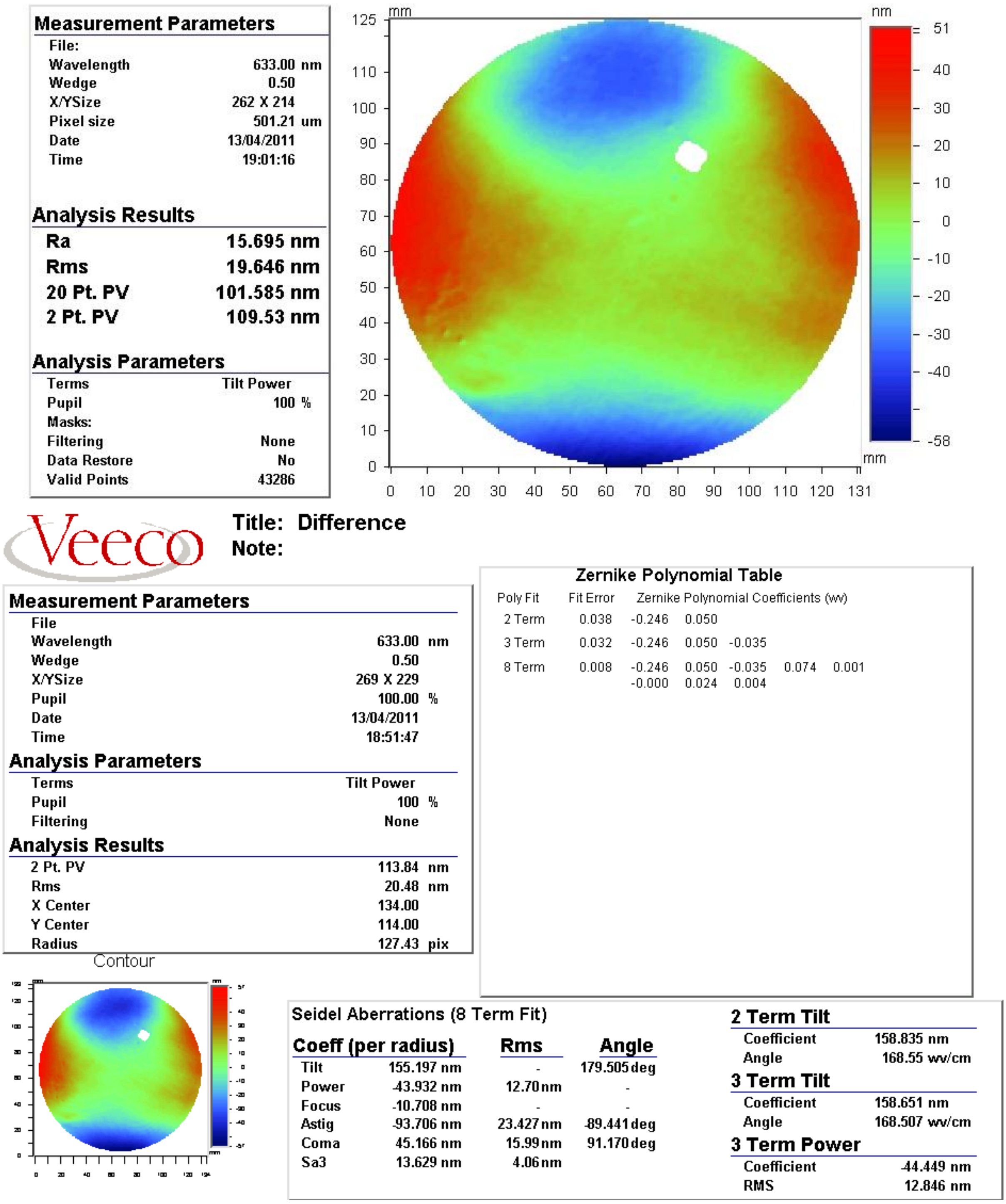

Figure 16. Results of the intereferometric analysis of the 2nd element of the EW.

End of document